Journal of Applied Mechanics and Technical Physics, Vol. 43, No. 3, pp. 415–423, 2002

UNSTEADY BEHAVIOR OF AN ELASTIC BEAM FLOATING ON SHALLOW WATER UNDER EXTERNAL LOADING

I. V. Sturova

UDC 532.591:539.3:534.1

A solution is derived for the two-dimensional unsteady problem of the behavior of an elastic beam of finite dimensions floating on the free surface of water under external loading. It is assumed that the fluid is ideal and incompressible and its depth is well below the beam length. The simultaneous motion of the beam and the fluid is considered within the framework of linear theory, and the fluid flow is assumed to be potential. The behavior of the beam under various loadings with and without allowance for the inertia of the load is studied.

Results of studies of the hydroelastic behavior of floating bodies (ice floes, breakwaters, and floating platforms) have broad applications. The behavior of an infinite ice floe under a moving external load has been studied in sufficient detail [1–3]. In addition, interest in the unsteady behavior of floating elastic structures has increased recently because of the design of floating platforms for various uses. These structures have great width and length and relatively small flexural rigidity; therefore, investigation of their hydroelastic behavior is of greater importance than studies of their motion as rigid bodies. The operation of these platforms requires determination of their dynamic durability with respect to the effect of unsteady external loading due to intense traffic, load movement, takeoffs and landings of airplanes, missile takeoffs, etc. Usually, these man-made structures are considered to be of a rectangular shape with a large ratio of length to width and a small ratio of thickness to length and width, and, hence, the platform is simulated as a thin elastic plate.

The solution of unsteady three-dimensional hydroelastic problems is a difficult task even for linear formulations and requires high computational cost [4]. In this paper, we propose a simplified model in which an elongated rectangular plate is replaced by an elastic beam, and the problem reduces to a two-dimensional one. The depth of the fluid is assumed to be smaller than the beam length, and the problem is solved in a shallow-water approximation.

1. Formulation of the Problem. Let an elastic beam of length $2L$ float on the surface of an ideal incompressible fluid layer of depth H. The surface of the fluid that is not covered with the beam is free. The fluid flow is assumed to be potential. The velocity potentials describing the fluid motion in the regions under the beam and outside the beam are denoted by $\varphi_1(x,t)$ and $\varphi_2(x,t)$, respectively (x is the horizontal coordinate, $x=0$ corresponds to the middle of the beam, and t is time).

A deflection of an Euler elastic beam $w(x,t)$ is described by the equation

$$D\,\frac{\partial^4 w}{\partial x^4}+\rho_1 h_1\,\frac{\partial^2 w}{\partial t^2}+g\rho w+\rho\,\frac{\partial\varphi_1}{\partial t}=-P(x,t)\quad(|x|\leqslant L),\tag{1.1}$$

where $D=Eh_1^3/[12(1-\nu^2)]$, E, ρ_1, h_1, and ν are the Young's modulus, density, thickness, and Poisson's ratio of the beam, respectively, ρ is the water density, and g is the acceleration of gravity. The function $P(x,t)$ can be a specified function, and it describes the external pressure acting upon the beam that is independent of the beam motion (so-called inertia-free loading). However, in the general case of the motion of a massive load on the beam, the inertial forces arising due to combined oscillations of this load and the beam (inertial loading) should be taken into account. In this case,

Lavrent'ev Institute of Hydrodynamics, Siberian Division, Russian Academy of Sciences, Novosibirsk 630090.
Translated from Prikladnaya Mekhanika i Tekhnicheskaya Fizika, Vol. 43, No. 3, pp. 88–98, May–June, 2002. Original article submitted January 9, 2002.

0021-8944/02/4303-0415 $27.00

$$P(x,t) = M\Big(g + \frac{\partial^2 w}{\partial t^2}\Big) Q(x,t), \tag{1.2}$$

where M is the linear load weight and $Q(x,t)$ is a specified function.

According to linear shallow-water theory, the following relation is valid:

$$\frac{\partial w}{\partial t} = -h\,\frac{\partial^2 \varphi_1}{\partial x^2} \quad (|x| \leqslant L), \qquad h = H - d. \tag{1.3}$$

Here $d = \rho_1 h_1/\rho$ is the draft of the beam.

In the free-water region, the velocity potential $\varphi_2(x,t)$ satisfies the equation

$$\frac{\partial^2 \varphi_2}{\partial x^2} = \frac{1}{gH}\,\frac{\partial^2 \varphi_2}{\partial t^2} \qquad (|x| > L). \tag{1.4}$$

The displacement of the free surface $\eta(x,t)$ is determined from the relation

$$\eta = -\frac{1}{g}\,\frac{\partial \varphi_2}{\partial t}. \tag{1.5}$$

It is also of interest to solve this problem under the assumption of a non-gravity fluid at $|x| > L$. This model is used in the theory of impact to study short-duration external action on a floating elastic body [5]. For a non-gravity fluid in the shallow-water approximation, we have the following equation instead of Eq. (1.4):

$$\varphi_2(x,t) = 0 \qquad (|x| > L). \tag{1.6}$$

If $|x| = L$, the following matching conditions (continuity of pressure and mass flow) must be satisfied:

$$\frac{\partial \varphi_1}{\partial t} = \frac{\partial \varphi_2}{\partial t}, \qquad \frac{\partial \varphi_1}{\partial x} = \frac{H}{h}\,\frac{\partial \varphi_2}{\partial x}. \tag{1.7}$$

At the edges of the beam, the free-edge conditions are satisfied, which imply that the bending moment and the shear force are equal to zero:

$$\frac{\partial^2 w}{\partial x^2} = \frac{\partial^3 w}{\partial x^3} = 0 \qquad (|x| = L). \tag{1.8}$$

We assume that at the initial time, the fluid and the beam are at rest:

$$w = \frac{\partial w}{\partial t} = \varphi_1 = \varphi_2 = \frac{\partial \varphi_2}{\partial t} = 0 \qquad (t = 0). \tag{1.9}$$

We seek the beam deflection $w(x,t)$, the free-surface displacement $\eta(x,t)$, and the velocity potentials $\varphi_{1,2}(x,t)$ as the sum of even and odd components over x. Then, the initial problem (1.1)–(1.5) and (1.7)–(1.9) is divided into two parts with respect to the corresponding components of the desired functions. In this case, the region for which the solution is sought can be reduced to the half-strip $x \geqslant 0$.

We convert to dimensionless variables (primed):

$$(x', H', h') = \frac{1}{L}\,(x, H, h), \quad t' = \sqrt{\frac{g}{L}}\,t, \quad (w', \eta') = \frac{1}{a}(w, \eta), \quad \varphi'_{1,2} = \frac{1}{a\sqrt{gL}}\,\varphi_{1,2}, \quad P' = \frac{P}{a\rho g}.$$

Here a is a multiplier that has the dimension of length. For inertial loading, we define the multiplier a as $a = M/(l\rho)$; $Q' = Q/l$ (l is the half-length of the loaded region). Then, we use the following dimensionless coefficients:

$$\alpha = \frac{a}{L}, \quad \beta = \frac{H}{h}, \quad \gamma = \frac{d}{L}, \quad \delta = \frac{D}{\rho g L^4}.$$

Below, the solution of the problem is derived for inertial loading, and a simpler solution for inertia-free loading can be considered as a particular case for $\alpha = 0$.

2. Even Part of the Solution. In the dimensionless variables (below, the primes are omitted), the initial problem for the even (symmetrical) components (denoted by the superscript s) has the form

$$\delta\,\frac{\partial^4 w^s}{\partial x^4} + \gamma\,\frac{\partial^2 w^s}{\partial t^2} + w^s + \frac{\partial \varphi_1^s}{\partial t} = -\Big(1 + \alpha\,\frac{\partial^2 w^s}{\partial t^2}\Big) Q(x,t),$$
$$\frac{\partial w^s}{\partial t} = -h\,\frac{\partial^2 \varphi_1^s}{\partial x^2} \quad (0 \leqslant x \leqslant 1); \tag{2.1}$$

$$\frac{\partial^2 \varphi_2^s}{\partial t^2} = H \frac{\partial^2 \varphi_2^s}{\partial x^2}, \quad \eta^s = -\frac{\partial \varphi_2^s}{\partial t} \quad (x > 1); \tag{2.2}$$

$$\frac{\partial w^s}{\partial x} = \frac{\partial \varphi_1^s}{\partial x} = 0 \quad (x = 0); \tag{2.3}$$

$$\varphi_1^s = \varphi_2^s, \quad \frac{\partial \varphi_1^s}{\partial x} = \beta \frac{\partial \varphi_2^s}{\partial x}, \quad \frac{\partial^2 w^s}{\partial x^2} = \frac{\partial^3 w^s}{\partial x^3} = 0 \quad (x = 1); \tag{2.4}$$

$$w^s = \frac{\partial w^s}{\partial t} = \varphi_1^s = \varphi_2^s = \frac{\partial \varphi_2^s}{\partial t} = 0 \quad (t = 0). \tag{2.5}$$

We seek the beam deflection $w^s(x,t)$ as an expansion over the even eigen-oscillations of the beam with free ends in vacuum:

$$w^s(x,t) = \sum_{n=1}^{\infty} a_n(t) \psi_n^s(x). \tag{2.6}$$

Here $\psi_n^s(x)$ is a solution of the spectral problem

$$\begin{gathered} \psi_n^{s\,(\mathrm{IV})} = (\lambda_n^s)^4 \psi_n^s \quad (0 \leqslant x \leqslant 1), \\ \psi_n^{s\,\prime} = 0 \quad (x = 0), \qquad \psi_n^{s\,\prime\prime} = \psi_n^{s\,\prime\prime\prime} = 0 \quad (x = 1). \end{gathered} \tag{2.7}$$

This solution has the following form (see, for example, [6]):

$$\begin{gathered} \psi_1^s(x) = 1/\sqrt{2}, \qquad \psi_n^s = D_n^s(\cos\lambda_n^s x + S_n^s \cosh\ \lambda_n^s x), \\ D_n = 1/\sqrt{1 + (S_n^s)^2}, \qquad S_n^s = \cos\lambda_n^s / \cosh\ \lambda_n^s \qquad (n \geqslant 2). \end{gathered} \tag{2.8}$$

The eigenvalues λ_n^s $(\lambda_{n+1}^s > \lambda_n^s)$ are determined from the dispersion relation $\tan\lambda_n^s = -\tanh\lambda_n^s$, $\lambda_1^s = 0$. The functions $\psi_n^s(x)$ form a full orthogonal system:

$$\int_{-1}^{1} \psi_n^s(x) \psi_m^s(x)\, dx = \delta_{mn}, \tag{2.9}$$

where δ_{mn} is the Kronecker symbol.

We substitute expansions (2.6) into the first equation (2.1) and initial conditions (2.5), multiply the obtained relations by $\psi_m^s(x)$, and integrate them over x from -1 to 1. Using the properties of the functions $\psi_m^s(x)$, we obtain the system of ordinary differential equations (a dot from above denotes derivation with respect to time)

$$\gamma \ddot{a}_m + [1 + \delta(\lambda_m^s)^4] a_m + f_m(t) = -\Big[Z_m(t) + \alpha \sum_{n=1}^{\infty} \ddot{a}_n(t) \chi_{mn}(t)\Big] \tag{2.10}$$

with the initial conditions

$$a_m(0) = \dot{a}_m(0) = 0. \tag{2.11}$$

Here

$$f_m(t) = \int_{-1}^{1} \frac{\partial \varphi_1^s}{\partial t} \psi_m^s(x)\, dx, \qquad Z_m(t) = \int_{-1}^{1} Q(x,t) \psi_m^s(x)\, dx, \qquad \chi_{mn}(t) = \int_{-1}^{1} Q(x,t) \psi_m^s(x) \psi_n^s(x)\, dx.$$

A solution for $\varphi_1^s(x,t)$ is sought in the form

$$\varphi_1^s(x,t) = -\frac{1}{h} \left(\sum_{n=1}^{\infty} \dot{a}_n(t) \Phi_n^s(x) + q^s(x,t) \right), \tag{2.12}$$

where the functions $\Phi_n^s(x)$ satisfy the equation

$$\Phi_n^{s\,\prime\prime}(x) = \psi_n^s(x) \tag{2.13}$$

and are written as

$$\Phi_1^s(x) = x^2/(2\sqrt{2}), \quad \Phi_n^s(x) = D_n^s(S_n^s \cosh\ \lambda_n^s x - \cos\lambda_n^s x)/(\lambda_n^s)^2 \quad (n \geqslant 2). \tag{2.14}$$

The function q^s is unknown and needs to be determined. According to Eq. (2.1), boundary condition (2.3), and initial condition (2.5), the function q^s depends only on time and satisfies the initial condition $q^s(0) = 0$. This function is determined from the matching condition for the potentials $\varphi_1^s(x,t)$ and $\varphi_2^s(x,t)$ and their derivatives with respect to x for $x = 1$. According to (2.4) and (2.12), we have

$$\varphi_2^s\Big|_{x=1} = -\frac{1}{h}\Big(\frac{\dot a_1(t)}{2\sqrt{2}} + q^s(t)\Big), \quad \frac{\partial \varphi_2}{\partial x}\Big|_{x=1} = -\frac{\dot a_1(t)}{H\sqrt{2}}. \tag{2.15}$$

The solution of the first equation in (2.2) with the second boundary condition in (2.15) and initial conditions (2.5) has the form

$$\varphi_2^s(x,t) = \begin{cases} a_1(t-(x-1)/\sqrt{H})/\sqrt{2H}, & (x-1)/\sqrt{H} < t < \infty, \\ 0, & 0 < t < (x-1)/\sqrt{H}. \end{cases}$$

Hence,

$$q^s(t) = -\frac{1}{\sqrt{2}}\Big(\frac{\dot a_1(t)}{2} + \frac{h a_1(t)}{\sqrt{H}}\Big), \quad f_m(t) = -\frac{1}{h}\sum_{n=1}^{\infty} \ddot a_n(t) C_{mn} + \frac{\ddot a_1(t)}{2h} + \frac{\dot a_1(t)}{\sqrt{H}}, \tag{2.16}$$

$$C_{mn}^s = \int_{-1}^{1} \psi_m^s(x)\Phi_n^s(x)\,dx.$$

With allowance for (2.8) and (2.14), we have

$$C_{11}^s = 1/6, \quad C_{1n}^s = C_{n1}^s = -2\sqrt{2}D_n^s \sin\lambda_n^s/(\lambda_n^s)^3,$$

$$C_{nm}^s = C_{mn}^s = 8D_n^s D_m^s(\lambda_m^s\cos\lambda_n^s\sin\lambda_m^s - \lambda_n^s\sin\lambda_n^s\cos\lambda_m^s)/((\lambda_n^s)^4 - (\lambda_m^s)^4)$$

$$(n \neq m, \quad n, m \geqslant 2),$$

$$C_{nn}^s = -2(D_n^s)^2\sin\lambda_n^s(\sin\lambda_n^s + \cos\lambda_n^s/\lambda_n^s)/(\lambda_n^s)^2.$$

Substitution of (2.16) into (2.10) yields the following system of ordinary differential equations (ODE) for determining the functions $a_n(t)$ subject to the initial conditions (2.11):

$$\sum_{n=1}^{\infty} \ddot a_n\Big(\gamma\delta_{mn} - \frac{C_{mn}^s}{h} + \frac{1}{2h}\,\delta_{1m} + \alpha\chi_{mn}(t)\Big) + \frac{\dot a_1}{\sqrt{H}}\,\delta_{1m} + a_m[1 + \delta(\lambda_m^s)^4] = -Z_m(t). \tag{2.17}$$

Once the $a_n^s(t)$ are determined, we can find all characteristics of the symmetrical motion of the fluid and the beam. For example, for $x > 1$, the displacement of the free surface of the fluid is equal to

$$\eta^s(x,t) = \begin{cases} -\dot a_1(t-(x-1)/\sqrt{H})/\sqrt{2H}, & (x-1)/\sqrt{H} < t < \infty, \\ 0, & 0 < t < (x-1)/\sqrt{H}. \end{cases}$$

Assuming that the fluid is non-gravity for $|x| > 1$ and using (1.6), we have

$$q^s(t) = -\dot a_1(t)/(2\sqrt{2});$$

in this case, in system (2.17), the term $\dot a_1\delta_{1m}/\sqrt{H}$ is omitted.

3. Odd Part of the Solution. The odd (antisymmetric) components (denoted by the superscript a) are solutions of Eqs. (2.1), (2.2), (2.4), and (2.5) with the boundary condition

$$w^a = \varphi_1^a = 0 \quad (x = 0).$$

The beam deflection $w^a(x,t)$ is sought as an expansion in the odd eigenfunctions:

$$w^a(x,t) = \sum_{n=1}^{\infty} b_n(t)\psi_n^a(x), \tag{3.1}$$

where $\psi_n^a(x)$ is a solution of an equation similar to (2.7) subject to the boundary conditions

$$\psi_n^a = 0 \quad (x = 0), \qquad \psi_n^{a\prime\prime} = \psi_n^{a\prime\prime\prime} = 0 \quad (x = 1).$$

The odd eigenfunctions have the form [6]

$$\psi_1^a(x) = \sqrt{3/2}\,x, \quad \psi_n^a(x) = D_n^a(\sin\lambda_n^a x + S_n^a \sinh\lambda_n^a x),$$
$$D_n^a = 1/\sqrt{1-(S_n^a)^2}, \quad S_n^a = \cos\lambda_n^a/\cosh\lambda_n^a \quad (n \geqslant 2). \tag{3.2}$$

The eigenvalues of λ_n^a are determined from the dispersion relation $\tan\lambda_n^a = \tanh\lambda_n^a$. The functions $\psi_n^a(x)$ also form a full orthonormal system and satisfy a relation similar to (2.9).

As is noted in Sec. 2, we have the system of ODE

$$\gamma\ddot{b}_m + [1+\delta(\lambda_m^a)^4]b_m + v_m(t) = -\Big(Y_m(t) + \alpha\sum_{n=1}^{\infty}\ddot{b}_n(t)\Lambda_{mn}(t)\Big)$$

with the initial conditions

$$b_m(0) = \dot{b}_m(0) = 0,$$

where

$$v_m(t) = \int_{-1}^{1}\frac{\partial\varphi_1^a}{\partial t}\,\psi_m^a(x)\,dx, \quad Y_m(t) = \int_{-1}^{1}Q(x,t)\psi_m^a(x)\,dx,$$

$$\Lambda_{mn}(t) = \int_{-1}^{1}Q(x,t)\psi_m^a(x)\psi_n^a(x)\,dx.$$

The solution for $\varphi_1^a(x,t)$ is sought in the form

$$\varphi_1^a(x,t) = -\frac{1}{h}\Big(\sum_{n=1}^{\infty}\dot{b}_n(t)\Phi_n^a(x) + q^a(x,t)\Big),$$

where the functions $\Phi_n^a(x)$ satisfy an equation similar to (2.13) and are written as

$$\Phi_1^a(x) = x^3/(2\sqrt{6}), \quad \Phi_n^a(x) = D_n^a(S_n^a\sinh\lambda_n^a x - \sin\lambda_n^a x)/(\lambda_n^a)^2 \quad (n \geqslant 2). \tag{3.3}$$

The function $q^a(x,t)$ must satisfy the equation

$$\frac{\partial^2 q^a}{\partial x^2} = 0$$

with the boundary condition $q^a(0,t) = 0$, hence,

$$q^a(x,t) = xu(t), \qquad u(0) = 0,$$

where $u(t)$ is an unknown function. Unlike in the symmetrical part of the solution, in determining $u(t)$ from the matching conditions for the potentials $\varphi_1^a(x,t)$ and $\varphi_2^a(x,t)$ and their derivatives with respect to x for $x = 1$, in the main system

$$\sum_{n=1}^{\infty}\ddot{b}_n\Big(\gamma\delta_{mn} - \frac{C_{mn}^a}{h} + \frac{1}{6h}\,\delta_{1m} + \alpha\Lambda_{mn}(t)\Big) + \frac{\dot{b}_1}{2\sqrt{H}}\,\delta_{1m} + b_m[1+\delta(\lambda_m^a)^4] + \sqrt{2/(3H)}\,u\delta_{1m} = -Y_m(t) \tag{3.4}$$

$$\Big(C_{mn}^a = \int_{-1}^{1}\psi_m^a(x)\Phi_n^a(x)\,dx\Big),$$

the following additional differential equation appears:

$$\dot{u} + hu/\sqrt{H} = -(\ddot{b}_1/\sqrt{3} + h\sqrt{3/H}\,\dot{b}_1)/(2\sqrt{2}).$$

With allowance for (3.2) and (3.3), we obtain

$$C_{11}^a = 1/10, \quad C_{1n}^a = C_{n1}^a = 2\sqrt{6}D_n^a(\cos\lambda_n^a - \sin\lambda_n^a/\lambda_n^a)/(\lambda_n^a)^3,$$

$$C_{nm}^a = C_{mn}^a = 8D_n^aD_m^a(\lambda_n^a\cos\lambda_n^a\sin\lambda_m^a - \lambda_m^a\sin\lambda_n^a\cos\lambda_m^a)/((\lambda_n^a)^4 - (\lambda_m^a)^4) \qquad (n \neq m, \quad n,m \geqslant 2),$$

$$C_{nn}^a = 2(D_n^a)^2\cos\lambda_n^a(\sin\lambda_n^a/\lambda_n^a - \cos\lambda_n^a)/(\lambda_n^a)^2.$$

For $x > 1$, the free-surface displacement has the form

$$\eta^a(x,t) = \begin{cases} -[u(\xi) + \sqrt{3}\dot{b}_1(\xi)/(2\sqrt{2})]/\sqrt{H}, & (x-1)/\sqrt{H} < t < \infty, \\ 0, & 0 < t < (x-1)/\sqrt{H}, \end{cases}$$

where $\xi = t - (x-1)/\sqrt{H}$.

Under the assumption of the fluid weightlessness for $|x| > 1$, the function $u(t)$ becomes

$$u(t) = -\dot{b}_1(t)/(2\sqrt{6}),$$

and the system of ODE reduces to system (3.4) in which the terms $b_1\delta_{1m}/(2\sqrt{H})$ and $\sqrt{2/(3H)}u\delta_{1m}$ are omitted.

4. Numerical Calculations. To test the computational algorithm, we used the solution of the problem of the effect of a periodic surface pressure on a floating elastic beam [7]. The external pressure distribution in dimensional variables was specified as

$$P(x,t) = a\rho g F(x) \sin \omega t; \qquad (4.1)$$

$$F(x) = \begin{cases} 1 - ((x-l_1)/l)^2, & |x - l_1| \leqslant l, \\ 0, & |x - l_1| > l \end{cases} \qquad (l,\ l_1 > 0,\ l_1 + l < L). \qquad (4.2)$$

The calculations performed for $l_1 = 0$ and $L/2$ and the dimensionless frequency $\omega\sqrt{H/g}$ in the range of 0.1–0.5 showed that the oscillations of the beam and the ambient fluid enter a steady periodical regime after approximately 2–3 oscillation periods $2\pi/\omega$. In the steady regime, the amplitudes of surface waves and beam deflections coincide with those obtained in [7].

To study unsteady inertia-free action on the beam, we chose an external load of the form

$$P(x,t) = a\rho g F(x) B(t), \qquad (4.3)$$

where the function $F(x)$ is defined by expression (4.2), and the time dependence has the form

$$B(t) = \begin{cases} t/b, & t \leqslant b, \\ 2 - t/b, & b \leqslant t \leqslant 2b, \\ 0, & t > 2b. \end{cases}$$

The initial parameters had the following values: $D = 4.476 \cdot 10^{10}$ kg $\cdot$ m^2/sec^2, $H = 20$ m, $\rho = 10^3$ kg/m^3, $d = 1$ m, $L = 200$ m, and $l = 40$ m. For these values, the dimensionless coefficients γ and δ are equal to $5 \cdot 10^{-3}$ and $2.852 \cdot 10^{-3}$, respectively.

To solve numerically the systems of ODE, we use the reduction method, and the infinite sets in (2.6) and (3.1) are replaced by finite sums with N terms. In all the calculations, $N = 10$, and further increase in N does not virtually affect the result.

The calculations for a beam of finite dimensions were compared with the well-known solution for an infinite beam (see, for example, [1, 2]). For loading in the form of (4.3), this solution has the form

$$w(x,t) = \frac{a\rho g}{\pi b} \int_0^\infty \frac{Y(k,t)\tilde{F}(k)\cos kx}{Dk^4 + \rho g}\, dk,$$

where

$$Y(k,t) = \begin{cases} \sin \Omega t/\Omega - t, & 0 \leqslant t \leqslant b, \\ [2\sin\Omega(b-t) + \sin\Omega t]/\Omega - 2b + t, & b \leqslant t \leqslant 2b, \\ [2\sin\Omega(b-t) - \sin\Omega(2b-t) + \sin\Omega t]/\Omega, & t > 2b, \end{cases}$$

$$\Omega^2(k) = hk^2(Dk^4 + \rho g)/(\rho + \rho_1 h_1 h k^2),$$

and $\tilde{F}(k)$ is the Fourier transform of the function $F(x)$ in (4.2):

$$\tilde{F}(k) = 4[\sin kl/(kl) - \cos kl]/(lk^2).$$

In the calculations whose results are given below it is assumed that $b = 0.5$ sec.

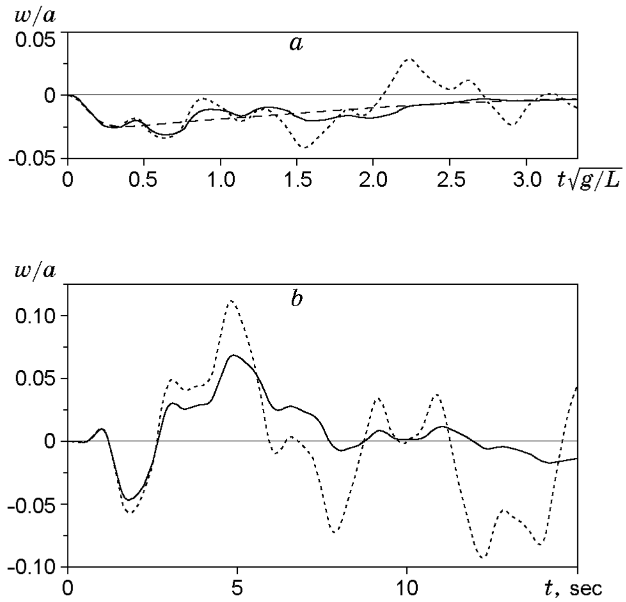

Fig. 1. Deflection of the beam versus time for loading in the form of (4.3) for $l_1 = 0$ and $x = 0$ (a) and $x = L$ (b): the solid curves refer to the solution for a finite beam and a gravity fluid, the dotted curves correspond to the solution for a finite beam and a non-gravity fluid, and the dashed curve refers to the solution for an infinite beam.

Figure 1 gives calculation results for symmetric external loading ($l_1 = 0$). The figure shows curves of deflections of the beam w/a versus dimensionless (a) and dimensional (b) time for $x = 0$ (solid curve in Fig. 1a) and $x = L$ (solid curve in Fig. 1b). For comparison, the corresponding solutions for a non-gravity fluid (dotted curves) are presented in Fig. 1a and b. The dashed curve in Fig. 1a shows the deflection of an infinite beam in the center of the applied pressure. We note that all three solutions coincide in the pressure epicenter during the time interval ($t \leqslant 2b = 1$ sec) in which this pressure acts; however, after the cessation of external loading, the deflections of the different beams considered differ significantly. The infinite beam tends monotonically to the initial state. The finite beam in a gravity fluid also enters the initial state but in a nonmonotonic manner. For the beam in a non-gravity fluid, the decrease in deflections with time both in the pressure epicenter and at the edges is not observed because in this case, the generation of surface waves and energy dissipation are absent.

The oscillations are significantly larger at the edges of the beam than in the pressure epicenter (compare Fig. 1a and Fig. 1b). The maximum deflection of the beam edge, observed at $t \approx 5$ sec, is almost twice that in the pressure epicenter.

The calculation results for asymmetric pressure application ($l_1 = 0.5L$) are shown in Fig. 2. This figure illustrates deflections in the pressure epicenter ($x = l_1$) for finite and infinite beams (solid and dotted curves in Fig. 2a). As in Fig. 1a, these solutions coincide at the moments when the pressure acts ($t \leqslant 1$ sec), and then, they gradually tend to zero. Figure 2b shows the oscillations of the beam edges at $x = L$ (solid curve) and $x = -L$ (dotted curve). The maximum deflections at the left and right edges of the beam are almost equal and virtually coincide with those in the symmetrical case (compare Fig. 1b and 2b). However, the maximum deflections appear at different times. First (at $t \approx 1.5$ sec), the maximum deflection is reached at the edge closest to the pressure region, and it is then (at $t \approx 4$ sec), reached at the opposite edge.

The effect of a moving inertial load is considered using an airplane landing as an example. It is assumed that at the initial time, the load has velocity v and touches the beam smoothly at the point $x = x_0$, and then it moves in a uniformly retarded manner to the left until a full stop at the point $x = x_1$ at the time $t = t_1 \equiv 2(x_0 - x_1)/v$. The load distribution over x is specified in the form of (4.2), where

$$l_1(t) = \begin{cases} x_0 - vt + v^2t^2/(4(x_0 - x_1)), & 0 \leqslant t \leqslant t_1, \\ x_1, & t > t_1. \end{cases} \tag{4.4}$$

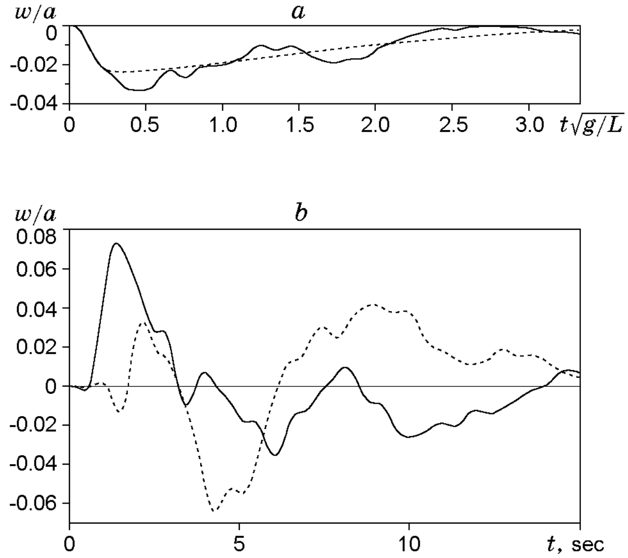

Fig. 2. Deflection of the beam versus time for loading in the form of (4.3) and $l_1 = 0.5L$: (a) $x = l_1$ (the solid curve refers to the solution for a finite beam and the dotted curve refers to an infinite beam); (b) the solution for a finite beam (the solid and dotted curves refer to $x = L$ and $-L$, respectively).

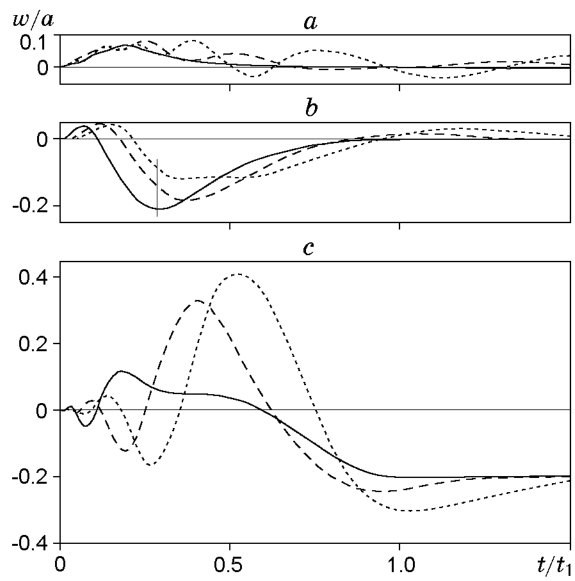

Fig. 3

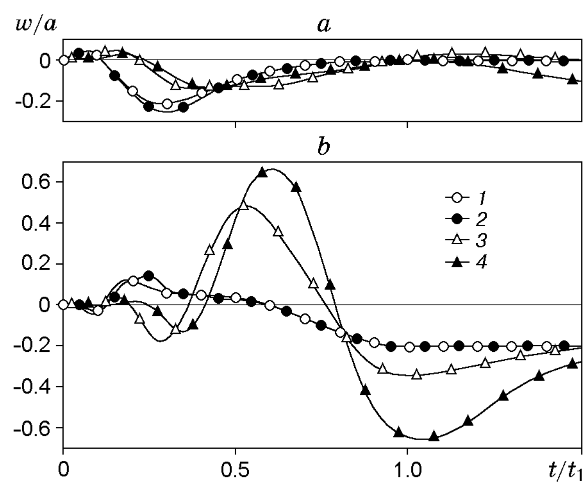

Fig. 4

Fig. 3. Deflection of the beam versus time for loading in the form of (4.5) for $\alpha = 0$ and $x = L$ (a), 0 (b), and $-L$ (c): the solid, dashed, and dotted curves refer to $v' = 0.1$, 0.3, 0.5, respectively.

Fig. 4. Deflection of the beam versus time for inertial loading in the form of (4.5) for $x = 0$ (a) and $-L$ (b): curves 1 refer to $v' = 0.1$ and $\alpha = 1$, curve 2 to $v' = 0.1$ and $\alpha = 10$, curves 3 to $v' = 0.5$ and $\alpha = 1$, and curves 4 to $v' = 0.5$ and $\alpha = 10$.

The function $Q(x, t)$ in (1.2) is specified as

$$Q(x, t) = [1 - \exp(-bt)]F(x, t)/l, \tag{4.5}$$

where $F(x, t)$ was defined in (4.2) with allowance for dependence (4.4) for $l_1(t)$. We used the previous initial parameters, except for $l = 0.1L$, $x_0 = 0.7L$, $x_1 = -0.7L$, and $b = 20/t_1$, which are adopted in this problem.

We first consider the behavior of the beam for $\alpha = 0$, i.e., ignoring the inertia of the load. Figure 3a–c shows deflections of the beam at the points $x = L$, 0, and $-L$ versus the initial velocity of load motion $v' \equiv v/\sqrt{gL} = 0.1$, 0.3, and 0.5 (solid, dashed, and dotted curves, respectively). We note that for the specified fluid depth, the dimensionless critical velocity of gravity and flexural–gravity waves is $\sqrt{H/L} \approx 0.33$. In Fig. 3b, the vertical line corresponds to the moment when the center of application of the load passes through the coordinate origin. It is obvious that the maximum beam deflection is reached at this moment only if the motion is rather slow. With increase in v', the maximum deflection at $x = 0$ decreases, and it appears after the load peak passes through the point $x = 0$. If $t > t_1$, the beam oscillations decay and gradually take the values corresponding to distributed static loading with center at the point $x = x_1$. The solution of this steady problem can be easily derived using the method described above: in this case, the systems of ODE (2.17) and (3.4) will reduce to simple systems of linear algebraic equations. The values of the dimensionless static deflection at $x = L$, 0, and $-L$ are equal to -0.003, -0.004, and -0.203, respectively.

Figure 3 shows that for the three points of the beam, the largest deflections arise, as a rule, on its left edge. An increase in the initial velocity of the load leads to larger oscillations of the beam and longer time of reaching a static regime compared with the time of motion of the load.

Figure 4a and b shows the beam deflections calculated with allowance for the inertial forces at $x = 0$ and $-L$ for $v' = 0.1$ (curves 1 and 2) and 0.5 (curves 3 and 4), respectively. Curves 1 and 3 correspond to $\alpha = 1$ and curves 2 and 4 to $\alpha = 10$. It can be seen that for a relatively low initial velocity $v' = 0.1$, an increase in the inertial parameter affects slightly the magnitude of deflections. However, for $v' = 0.5$, an increase in the coefficient α leads to larger deflections of the beam than those in the inertia-free case.

Conclusions. The results obtained show that the limited dimensions of the elastic beam has a significant effect on its behavior under unsteady loading. As was noted previously for periodic external loading [7], in some cases, the amplitudes of deflections of the beam at its edges far exceed the corresponding values for the middle region of the beam. Studies of the effect of the oscillatory inertial forces of the load support the conclusions in [1, 3] that the inertia of the load must be taken into account only for massive loads moving with large accelerations.

This work was supported by Integration Project No. 1 of the Siberian Division of the Russian Academy of Sciences, the Foundation for Leading Scientific Schools (Grant No. 00-15-96162), and the Russian Foundation for Fundamental Research (Grant No. 02-01-00739).

REFERENCES

1. D. Ye. Kheysin, *Dynamics of Floating Covers* [in Russian], Gidrometeoizdat, Leningrad (1967). (Technical Translation FSTC-HT-23-485-69, U.S. Army Foreign Science and Technology Center.)
2. L. V. Cherkesov, *Surface and Internal Waves* [in Russian], Naukova Dumka, Kiev (1973).
3. V. A. Squire, R. J. Hosking, A. D. Kerr, and P. J. Langhorne, *Moving Loads on Ice Plates*, Kluwer, Dordrecht (1996).
4. M. Kashiwagi, "A time-domain mode-expansion method for calculating transient elastic responses of a pontoon-type VLFS," *J. Mar. Sci. Technol.*, **5**, No. 2, 89–100 (2000).
5. A. Korobkin, "Unsteady hydroelasticity of floating plates," *J. Fluids Struct.*, **14**, 971–991 (2000).
6. A. P. Filippov, *Oscillations of Deformable Systems* [in Russian], Mashinostroenie, Moscow (1970).
7. I. V. Sturova, "Effect of periodic surface pressures on a floating elastic plate," *Prikl. Mat. Mekh.*, **66**, No. 1, 75–86 (2002).